Marine Geology 278 (2010) 43–53

Contents lists available at ScienceDirect

Marine Geology

journal homepage: www.elsevier.com/locate/margeo

Late Pleistocene–Holocene sedimentation surrounding an active seafloor gas-hydrate and cold-seep field on the Northern Gulf of Mexico Slope

Wesley C. Ingram [a,*], Stephen R. Meyers [b,1], Charlotte A. Brunner [c], Christopher S. Martens [a]

[a] Department of Marine Sciences, University of North Carolina-Chapel Hill, Chapel Hill, NC 27599, USA
[b] Department of Geological Sciences, University of North Carolina-Chapel Hill, Chapel Hill, NC 27599, USA
[c] Department of Marine Science, University of Southern Mississippi, Stennis Space Center, MS 39529, USA

ARTICLE INFO

Article history:
Received 6 April 2010
Received in revised form 31 August 2010
Accepted 4 September 2010
Available online 16 September 2010

Communicated by J.T. Wells

Keywords:
gas hydrate(s)
cold or petroleum seep(s)
Mississippi Canyon 118 (MC118)
National Gas Hydrate Seafloor Observatory
Gulf of Mexico
Late Pleistocene
Holocene
sedimentation
X-ray fluorescence
AMS ^{14}C dating

ABSTRACT

A chronostratigraphic framework is constructed from sediments surrounding an active gas-hydrate and cold-seep field, situated on the northern Gulf of Mexico slope within federal offshore lease block Mississippi Canyon 118 (MC118). Accelerator mass spectrometer (AMS) radiocarbon dating, foraminiferal biostratigraphy and nannofossil biostratigraphy are used to constrain the age of sediments from 10 gravity cores collected around the field. X-ray fluorescence (XRF) core scanning is employed to develop continuous down-core elemental profiles, which are used to evaluate biogenic calcium and siliciclastic titanium sediment inputs, and provide a means to correlate sediments across the study area and infer changes in sedimentation through time.
Spatial reconstruction of sedimentation surrounding the field indicates the following: (1) a consistent pattern of stratigraphic thinning in close proximity to the field over the past 14,000 yrs and (2), temporal changes in sedimentation that primarily reflect deglacial sea-level rise as well as regional factors such as Mississippi delta lobe switching. These results highlight the variability of sedimentation along a continental slope setting where marine cold seeps and gas hydrate persist, yet do not suggest slope failure or destabilization of the seafloor at this site, at least during the past 14,000 yrs. The evaluation of sedimentation at this location provides an important context for ongoing biogeochemical and geophysical monitoring of the MC118 site, which has been designated the first National Gas Hydrate Seafloor Observatory by the Gulf of Mexico Hydrate Research Consortium.

Published by Elsevier B.V.

1. Introduction

Marine gas hydrate formation represents an important process that can influence sedimentation in continental slope settings, and potentially contributes to continental margin slope failures on geologic time scales (Paull et al., 1996, 2003; Maslin et al., 1998, 2004; Haq, 1998; Mienert et al., 2005). The rapid dissociation of gas hydrates has also received much attention as a driver of past climate change, due to the potency of methane as a greenhouse gas, and the potential for destabilization of large hydrate deposits (e.g., Dickens et al., 1997; Katz et al., 1999; Kennett et al., 2000, 2003). In addition, gas-hydrate deposits and natural-gas/petroleum seepage at the seafloor are a shallow depth hazard for deep-water petroleum exploration (Solheim et al., 2005). As a consequence, all offshore blocks leased to the petroleum industry must undergo an extensive shallow hazard assessment and site survey of the seafloor prior to any operations, to mitigate the risk of unintended hydrate degassing or disturbances to the seafloor biological communities often present at these sites.

This study investigates sediments surrounding a gas-hydrate/cold-seep field within the Mississippi Canyon offshore federal lease block 118 (MC118) (Fig. 1) and is a component of a larger multi-disciplinary consortium effort to study the MC118 field (e.g., Sassen et al., 2006; Lutken et al., 2006; Sleeper et al., 2006; Sleeper and Lutken, 2008; Brunner 2007a; Lapham et al., 2008, in press). The MC118 site has been designated as the first National Gas Hydrate Seafloor Observatory by the Gulf of Mexico Hydrate Research Consortium jointly funded by NOAA, DOE and MMS (McGee, 2006). Several inter-related objectives specific to the MC118 field are addressed by this study and include the following: (1) to document the spatial and temporal variability of sedimentation surrounding the MC118 field during the late Pleistocene and Holocene, (2) to investigate the spatial scale over which processes associated with gas hydrates and cold seepage influence sedimentation, seafloor erosion, mass wasting and seabed morphology (e.g., Maslin et al., 1998, 2004; Paull et al., 1996, 2003; Mienert et al., 2005), and (3) to evaluate the sensitivity of

* Corresponding author. Devon Energy Corporation, 20 N. Broadway, Oklahoma City, OK 73102-8260, USA. Tel./fax: +1 405 228 8326.
E-mail addresses: wesley.ingram@dvn.com (W.C. Ingram), smeyers@geology.wisc.edu (S.R. Meyers), charlotte.brunner@usm.edu (C.A. Brunner), cmartens@email.unc.edu (C.S. Martens).
[1] Present address: Department of Geoscience, University of Wisconsin-Madison, Madison, WI 53706, USA.

0025-3227/$ – see front matter. Published by Elsevier B.V.
doi:10.1016/j.margeo.2010.09.002

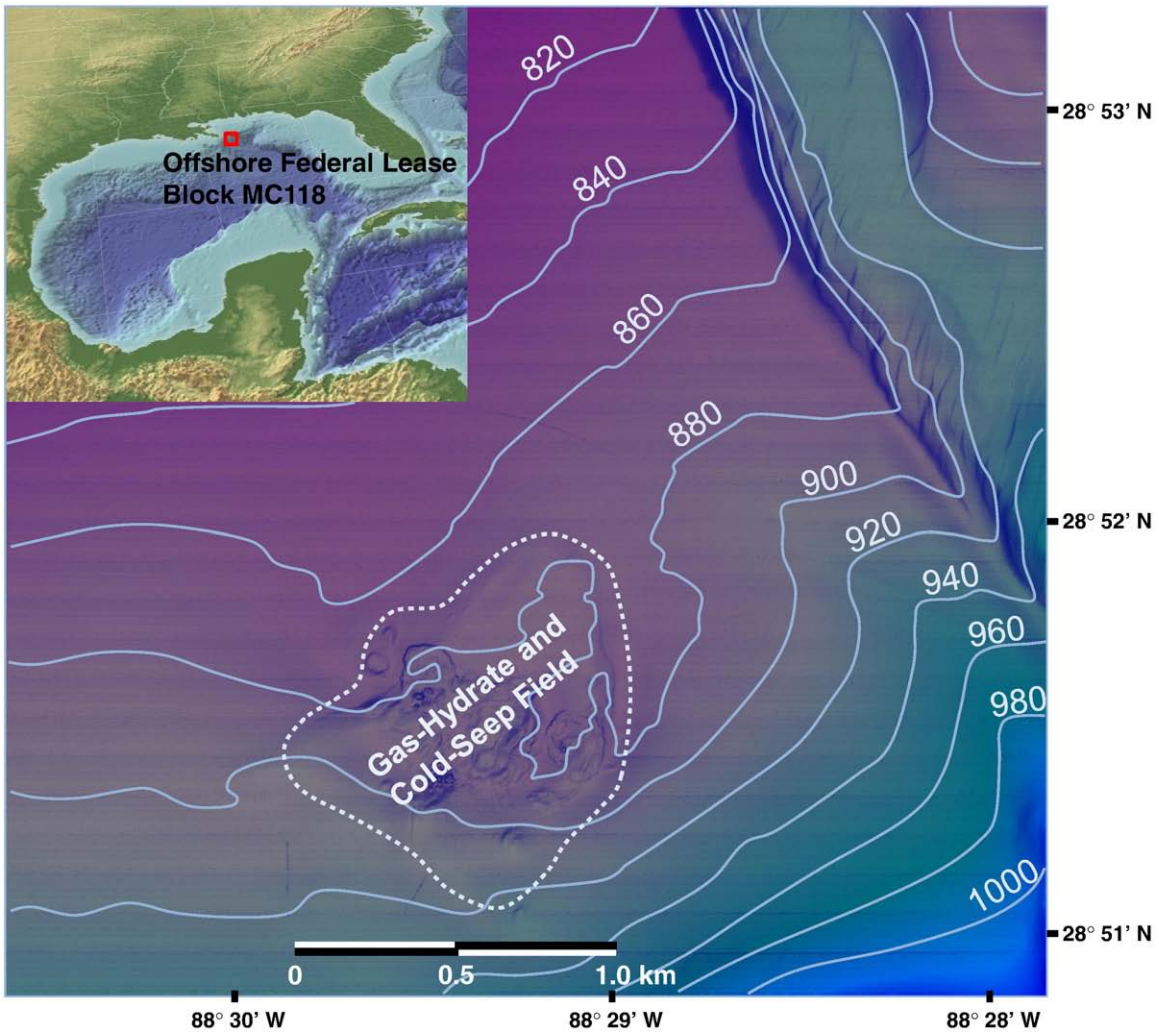

Fig. 1. Bathymetric map of the study area (Block MC118) with labeled contours (light blue) in meters water depth (e.g., Sleeper and Lutken, 2008) with inset digital elevation and bathymetry map (top left; cropped NOAA geophysical data center image) of the Gulf of Mexico region. Bathymetry provided by the Gulf of Mexico Hydrate Research Consortium, modified after the figure from Ken Sleeper. The location of MC118 offshore federal lease block is indicated by the red box in the inset map. The extent of the studied gas-hydrate–cold-seep field is outlined by the light blue dashed line and is characterized by an area with gas vents, seafloor pockmark features, petroleum seepage, shallow faults, carbonate hard-grounds and gas hydrate deposits. The study area is approximately 100 miles South of Gulfport Mississippi in 800 to 1000 m water depth.

sedimentation at the site to processes such as seafloor warping due to salt tectonics (e.g., Galloway et al., 2000; Winker and Booth, 2000; Diegel et al., 1995 Jackson, 1995), changes in sea level, Mississippi delta lobe switching, and other regional/global processes that have potentially influenced sediment accumulation and redistribution during the latest Pleistocene and Holocene.

Ten sediment gravity cores, collected during two separate cruises, have been collected around the gas-hydrate/cold-seep field to investigate sediments within the MC118 block and possible sedimentation disturbances in proximity to the field (Fig. 2). Biostratigraphic, sedimentologic and X-ray fluorescence core scanning analyses are used to define unique sedimentary packages, and chronologic control is achieved using biostratigraphy and AMS ^{14}C dating. Correlative horizons are utilized to construct sedimentation and isopach maps at various time intervals for the past 14,000 yrs. The comparison of sediment thicknesses and sedimentation rates surrounding the MC118 field (upslope and downslope) provides a means to infer processes that influence sedimentation at the seafloor in this location, and aids in the interpretation of the Late Pleistocene and Holocene depositional history at the MC118 site.

2. Geological setting: MC118

The bathymetry of the Gulf of Mexico continental slope is heavily influenced by the extensive Louann (Jurassic in age) subsurface salt formation (e.g., Diegel et al., 1995; Jackson, 1995; Galloway et al., 2000). Deformation of the salt through time has contributed to the present-day hummocky bathymetry of the northern Gulf of Mexico slope. On a local scale, movement of subsalt deposits may generate shallow faults that extend up to the seafloor, thereby providing migration pathways for hydrocarbons sourced by leaky oil and gas reservoirs at depth. As a consequence, there are numerous deep-water petroleum seeps, gas vents, methane cold seeps and thermogenic gas-hydrate fields within the Gulf of Mexico (Sassen et al., 2001). Hydrocarbons are rapidly cycled and oxidized in shallow sediments at these sites (Castellini et al., 2006). In particular, gas hydrates of a thermogenic origin form where upward-migrating hydrocarbon-rich fluids and gasses encounter cool bottom water temperatures (Milkov and Sassen, 2002).

A gas-hydrate/cold-seep field centered at 28.8523°N and 88.4920°W lies in approximately 890 m water depth within the

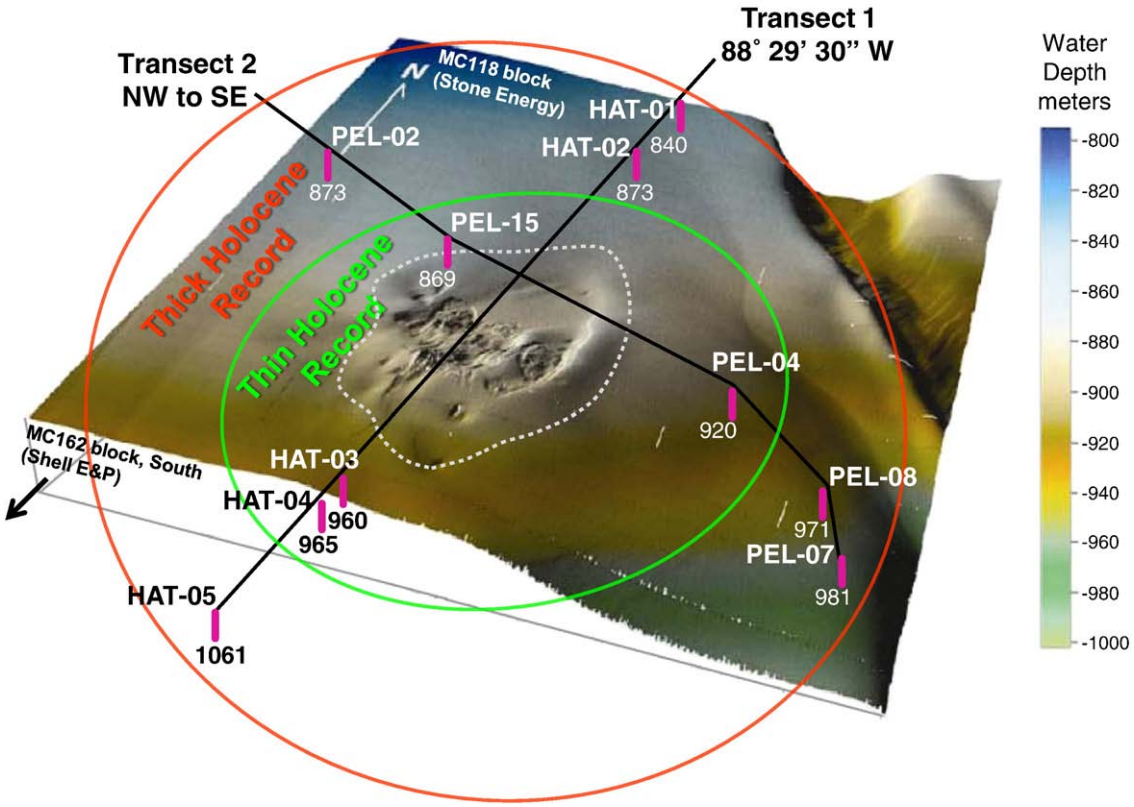

Fig. 2. Bathymetric map of the study site with the location of cores collected during cruises on the *R/V Hatteras* and *R/V Pelican*; base map image is courtesy of the Gulf of Mexico Hydrate Research Consortium (e.g., Sleeper et al., 2006). Cores are indicated as vertical magenta lines, with core identification (above) and water depth (in meters) below the core symbol. The edge of the gas-hydrate–cold-seep field is outlined by a thin dashed white line, black lines connecting cores indicate transects taken by the *R/V Hatteras* (Transect 1) and *R/V Pelican* (Transect 2). Cores within the green circle near the field exhibit a thin Holocene section, and cores outside the green circle and within the orange circle show a thicker Holocene section. The color bar on the far right indicates water depth.

MC118 offshore block (Figs. 1 and 2). Visible outcroppings of gas hydrates, faulted carbonate "hard-grounds" and pockmark features consistent with gas and petroleum seepage (e.g., Figs. 1 and 2) cover approximately 1 km^2 of the seafloor (e.g., Sassen et al., 2006; Sleeper et al., 2006). The seaward slope across the study area typically ranges from 3° to 4°, but slopes of 10° to 12° are present locally across pockmark features (Sleeper et al., 2006). The field is underlain by diapiric salt 200 to 300 m below the seafloor, which contributes to subsurface fluid migration, seafloor warping and irregular bathymetry at the site (Sassen et al., 2006). The supply of hydrocarbons (natural gas and petroleum) to the seafloor supports an active biological seep community (e.g., Sassen et al., 2006) and microbial chemolithotrophy in the immediate vicinity of active gas–fluid seepage.

Table 1
Cores collected at MC118 during cruises on the *R/V Hatteras* and *R/V Pelican*.

Date core taken	Aug. 2007	Aug. 2007	Aug. 2007	Aug. 2007	Aug. 2007
Cruise (research vessel)	*Hatteras*	*Hatteras*	*Hatteras*	*Hatteras*	*Hatteras*
Core I.D.	HAT-01	HAT-02	HAT-03	HAT-04	HAT-05
Core locations					
Latitude (N)	28 52′ 10.0″	28 51′ 50.0″	28 50′ 29.5″	28 50′ 29.3″	28 50′ 28.3″
Longitude (W)	88 29′ 30.0″	88 29′ 30.0″	88 29′ 30.0″	88 29′ 30.0″	88 29′ 30.0″
Water depth (m)	840	873	960	965	1061
Gross thickness					
Sub-bottom depth (cm)	226	275	272	283	269
Net thickness (cm)	222	261	258	282	255
Date core taken	April 2008	April 2008	April 2008	April 2008	April 2008
Cruise (research vessel)	*Pelican*	*Pelican*	*Pelican*	*Pelican*	*Pelican*
Core I.D.	PEL-02	PEL-15	PEL-04	PEL-07	PEL-08
Core locations					
Latitude (N)	28 51′ 34.0″	28 50′ 59.6″	28 50′ 49.5″	28 50′ 42.8″	28 50′ 37.7″
Longitude (W)	88 30′ 16.2″	88 29′ 37.5″	88 28′ 23.6″	88 27′ 53.3″	88 27′ 49.1″
Water depth (m)	873	869	920	981	971
Gross thickness					
Sub-bottom depth (cm)	440	460	405	600	711
Net thickness (cm)	438	445	400	597	703

List of gravity cores taken from 2 separate cruises, their location, water depth, sediment recovery and core labels.

3. Methods

3.1. Core collection

Gravity coring was conducted from the surface ships *R/V Hatteras* in August 2007 and *R/V Pelican* in April 2008. Five sediment gravity cores were recovered during the *R/V Hatteras*, in a depositional dip orientation, oriented along 88°29′30″ W (Fig. 2; Table 1). Coring operations onboard the cruise encountered "hard-grounds" at one location (failed core site) adjacent to the field resulting in recovery of only a few carbonate nodules. Five additional cores were recovered along the *Pelican* transect in a NW to SE orientation across the field (Fig. 2; Table 1). Small amounts of gas-hydrate cement were recovered during coring onboard the *Pelican* along the flanks of the field (Sleeper and Lutken, 2008; Fig. 1).

3.2. Core processing

After transport of the sediment cores to a land-based laboratory at the University of North Carolina, Chapel Hill, cores were split and prepared for sedimentological, biostratigraphic and geochemical analyses. One half of the split core was prepared for X-ray fluorescence scanning by applying a thin (4 μm) Ultralene film across the top of the sediment surface. The remaining material was described visually (Fig. 3) and then used for destructive sampling. All core material was placed in sealed plastic core sleeves and D-tubes, and stored in the core laboratory refrigerator at ~3 °C.

3.3. X-ray fluorescence core scanning

X-ray fluorescence (XRF) core scanning was used to evaluate down-core changes in the bulk geochemical composition of MC118 sediments, specifically focusing on calcium and titanium (Figs. 4 and 5) as measures of biogenic and terrigenous clastic sediment inputs, respectively. Split cores were analyzed using an Avaatech XRF core scanner with an Oxford 50 W X-ray source (rhodium target), and a Canberra X-PIPS detector with a 1500-micrometer silicon crystal. Continuous down-core X-ray fluorescence core scanning was conducted at a 1-cm resolution.

Calcium was measured using a 5 kV source voltage, 900 mA, without a filter, using a 90 s measurement time. Titanium was measured using a 10 kV source voltage, 1000 mA, with a cellulose filter, using a 90 s measurement time. To measure error and reproducibility, duplicate scans were performed at a 10-cm resolution using the same scanning parameters yielding highly reproducible results, with an average error less than 5%.

3.4. Foraminiferal biostratigraphy

A detailed planktonic foraminiferal biostratigraphy was performed on Core HAT-03 (Figs. 3 and 6). A total of 29 samples each at ~40 cm^3 were taken at 10-cm or less depth intervals and prepared for microscopic examination of the sand-size fraction. Sediment samples were dried at 50 °C for 48 h, soaked in a 1% Calgon solution to disaggregate clay-rich sediment, and washed on a screen with 63-μm openings until only the sand-sized fraction remained. The sand-size residue was examined for foraminifera under a (90×) Olympus SZX12 dissecting microscope. The Gulf of Mexico biostratigraphy of Kennett and Huddlestun (1972) was applied as modified by Kennett et al. (1985).

Several key biostratigraphic boundaries, Y/Z ~ 10 Ka and Y_1/Y_2 ~ 15 Ka calendar kilo-yrs BP, respectively (Flower and Kennett, 1990), were identified and used for age control in this core. Biostratigraphic boundaries used in this study are based partly on the disappearance of *Globorotalia inflata* and the reappearance of the *G. menardii plexus*, which correspond to sea-level and temperature changes in the Gulf of Mexico during deglaciation and the subsequent interglacial period (Flower and Kennett, 1990).

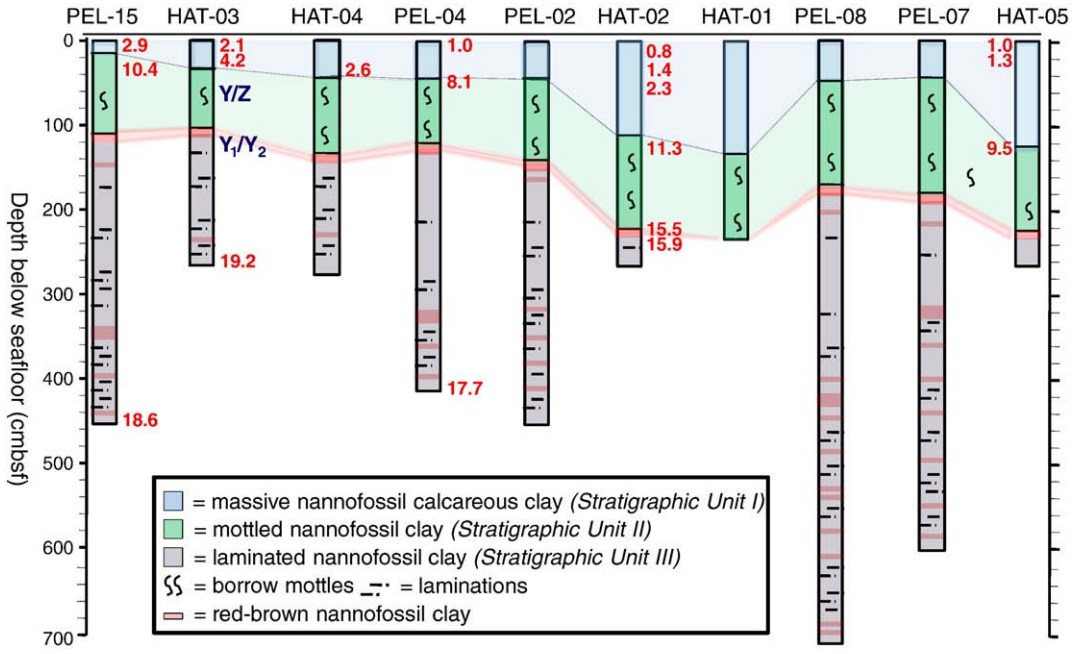

Fig. 3. Stratigraphic correlation of marine sediments collected in this study. Cores are arranged by increasing distance (left to right) from the gas-hydrate–cold-seep field. Dates obtained via AMS radiocarbon analysis of planktonic foraminifera (red, Ka) and foraminiferal biostratigraphic boundaries (dark blue, Y/Z ~ 10 Ka and Y_1/Y_2 ~ 15 Ka) are shown alongside their stratigraphic position; all reported ages are in calendar kilo-yrs BP. Three distinct stratigraphic units (see Results for detailed sedimentological descriptions) are identified as follows: Unit I (light blue) = massive nannofossil calcareous silty clay; Unit II (light green) = mottled nannofossil clay; Unit III (gray) = laminated nannofossil clay containing reddish-brown nannofossil clay layers (red lines). A distinct ~5-cm thick reddish clay layer with highly "reworked" (pre-Quaternary) nannofossils defines the top of Unit III.

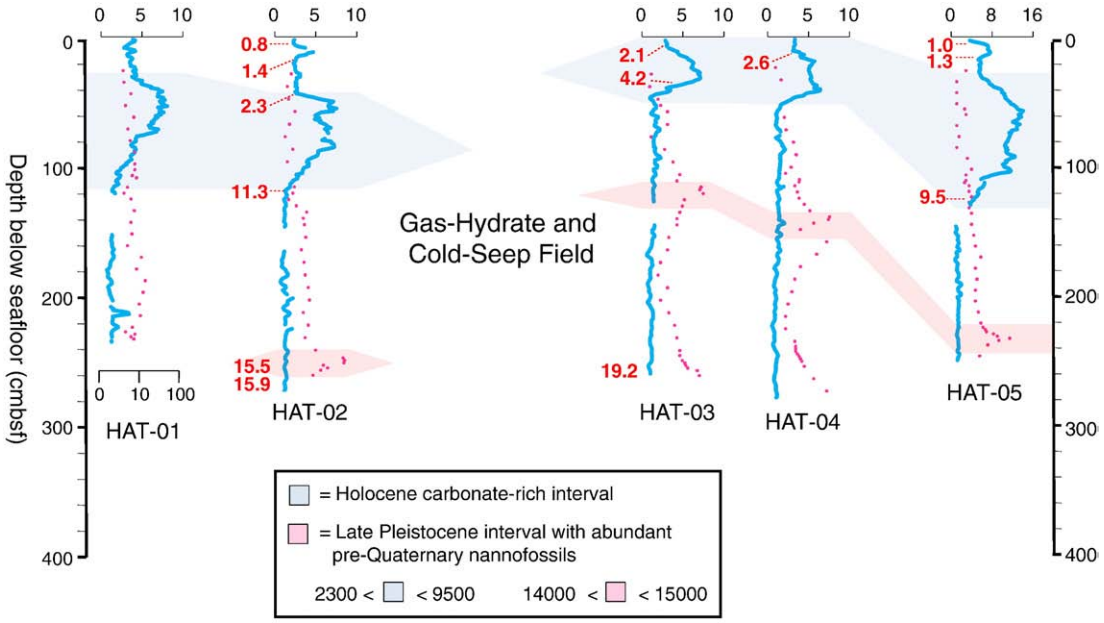

Fig. 4. X-ray fluorescence (XRF) core scanning Ca/Ti results (blue line), and the percentage of reworked nannofossils (red dots), for cores collected on the *R/V Hatteras* (Transect 1). The Ca/Ti data is plotted as a 3-cm moving average, and the reworked nannofossil data are plotted on a log scale (1 to 100%) shown at the bottom of the Core HAT-01. Two correlative horizons are identified as discussed in the text: a Holocene (Unit IA; 2300–9500 yrs) $CaCO_3$-rich interval (blue) and late Pleistocene (14,000–15,000 yrs) reworked nannofossil interval (red). The stratigraphic locations of radiocarbon in Ka (calendar kilo-yrs BP), are shown alongside each XRF profile.

3.5. Nannofossil biostratigraphy

An unconventional nannofossil biostratigraphy was performed on the cores at MC118 in an effort to tie into a previously documented chronology from the Orca Basin in the Gulf of Mexico (Fig. 6). The Orca Basin is an anoxic salt mini-basin that is ~290 km southwest of the Mississippi Delta at 2300 m water depth. The depression is a natural sediment catch with high sedimentation rates and no bioturbation, yielding a detailed sedimentary record, and providing isotopic and biostratigraphic evidence for deglacial flooding events into the Gulf of Mexico during the Late Pleistocene and Holocene transition (e.g., Marchitto and Wei, 1995; Kennett et al., 1985; Broecker et al., 1988,

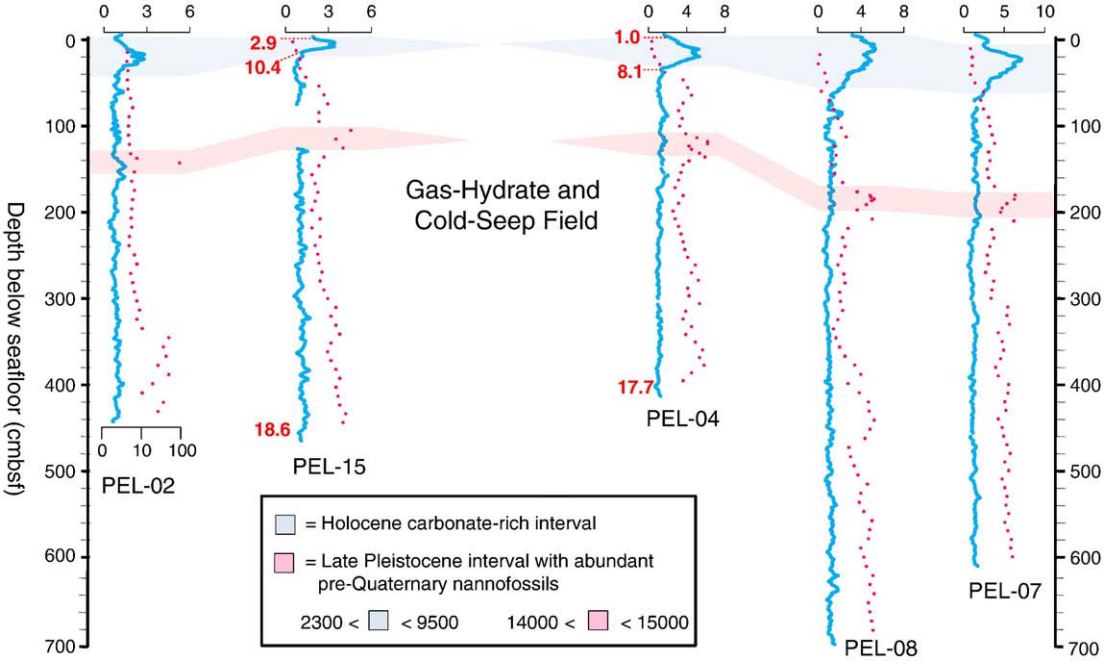

Fig. 5. X-ray fluorescence (XRF) core scanning Ca/Ti results (blue line), and the percentage of reworked nannofossils (red dots), for cores collected on the *R/V Pelican* (Transect 2). The Ca/Ti data is plotted as a 3-cm moving average, and the reworked nannofossil data are plotted on a log scale (1 to 100%) shown at the bottom of the Core PEL-02 on far left. Two correlative horizons are identified as discussed in the text: a Holocene (Unit IA; 2300–9500 yrs) $CaCO_3$-rich interval (blue) and late Pleistocene (14,000–15,000 yrs) reworked nannofossil interval (red). Radiocarbon ages are in Ka (calendar kilo-yrs BP).

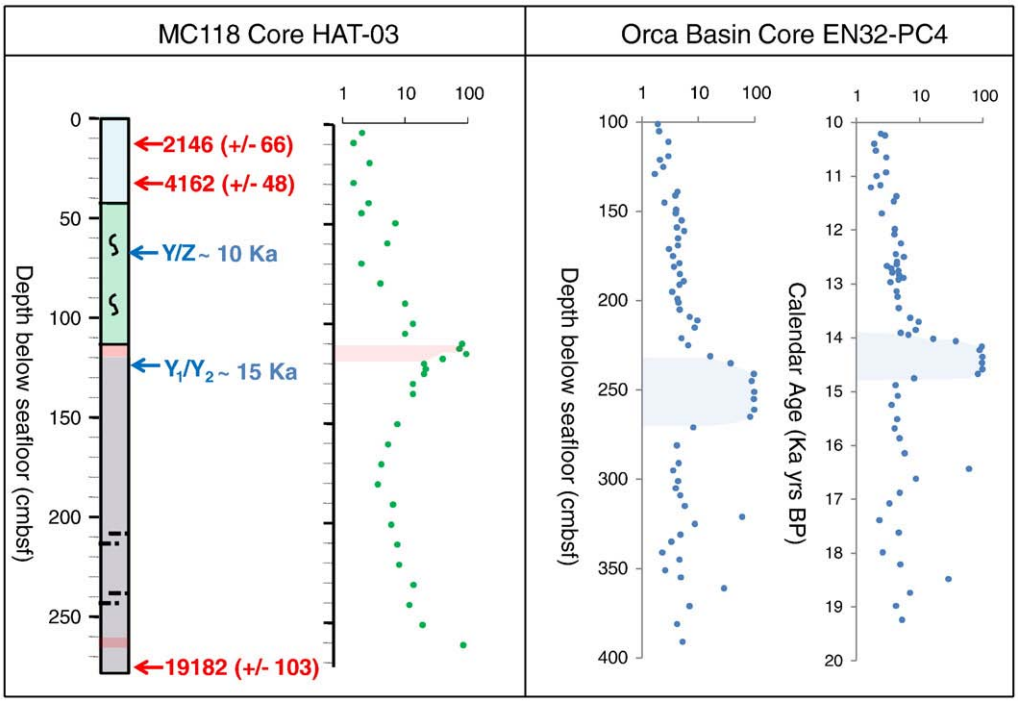

Fig. 6. Percentage of reworked nannofossils for MC118 (left panel) and the Orca Basin (right panel; data from Marchitto and Wei, 1995). The original Marchitto and Wei (1995) timescale for the EN32-PC4 core, derived from Flower and Kennett (1990) includes a 400-yr reservoir correction already applied to their radiocarbon ages. It is converted here to calendar kilo-yrs BP using the Fairbanks et al. (2005) calibration. This previous work places the most prominent peak of reworked nannofossils between 14 and 15 Ka calendar kilo-yrs BP. Age control for Core HAT-03 includes AMS radiocarbon ages (red), in calendar yrs BP, and foraminiferal biostratigraphic boundaries (dark blue, Y/Z ~ 10 Ka and Y_1/Y_2 ~ 15 Ka), also in calendar kilo-yrs BP. The age of the highly reworked nannofossil interval, constrained by biostratigraphy and radiocarbon age dates, is between 14,000 and 15,000 calendar kilo-yrs BP. Hence, the initial shallow peak of reworked nannofossils in Core HAT-03 (left plot) is coincident in age with the peak identified in Core EN32-PC4 (far right plot). Percentage of reworked nannofossils is plotted on a log scale in all three profiles.

1989; Flower and Kennett, 1990). Marchitto and Wei (1995) discovered an increase in the abundance of reworked (pre-Quaternary) nannofossils at the Orca Basin during meltwater pulse 1a (between 14 and 15 Ka), which they attributed to scouring of epicontinental sediments by glacial meltwater outflow down the Mississippi River drainage basin and into the Gulf of Mexico. A similar biostratigraphic "event" of highly reworked nannofossils was also observed in cores from the MC118 study area (Fig. 6).

Analysis of the percentage of reworked nannofossils in MC118 sediments followed the procedure of Marchitto and Wei (1995). Samples were taken at variable stratigraphic resolution to focus on intervals that tie into the Orca Basin record, yet were always less than 10-cm spacing. Sample smear slides were prepared from the unlithified marine sediments, and cover slips were mounted to slides using Norland-81 optical adhesive. Slides were viewed at 1250× on a Zeiss Axioscope under cross-polarized light. A total of at least 750 nannofossils were identified and counted in each sample. The percent reworked was obtained by counting the number of Pre-Quaternary nannofossils relative to the total number in a sample of at least 750; this ratio multiplied by 100 yielded the percent reworked, plotted on a log scale (Figs. 4, 5 and 6). The vast majority of the reworked (Pre-Quaternary) nannofossils are Cretaceous in age.

3.6. Radiocarbon dating

Planktonic foraminifera were picked for AMS radiocarbon dating to provide chronologic constraints for the recovered sediments. A total of 20 AMS radiocarbon dates were obtained from six different cores at various stratigraphic horizons with a focus on constraining the age of key correlative horizons, e.g., the $CaCO_3$-rich and reworked nannofossil interval (see Results section; Figs. 3–5). Approximately 5 mg of foraminiferal tests, mostly the white variety of *Globigerinoides ruber*, were handpicked from sieved sediment samples (see Foraminiferal biostratigraphy section). Microfossil tests were then sonicated in deionized water prior to processing for radiocarbon analysis.

Radiocarbon dating was performed by the National Ocean Science Accelerator Mass Spectrometry Facility (NOSAMS) at Woods Hole Oceanographic Institute. $\delta^{13}C$ values were determined to correct for fractionation effects. NOSAMS reports ages according to the convention outlined by Stuiver and Polach (1977) and Stuiver (1980). Radiocarbon ages are calculated using a 5568 yr half-life of radiocarbon and are reported by NOSAMS without reservoir corrections or calibration to calendar years. The provided radiocarbon ages were converted to calendar years before present (BP) using a recently updated calibration curve spanning 0 to 50,000 yrs from Fairbanks et al. (2005). A 400-year reservoir correction was applied to each radiocarbon age prior to conversion to calendar years, as utilized in previous investigations also using planktonic foraminifera of similar age in the Gulf of Mexico (e.g., Richey et al., 2007).

3.7. Isopach mapping

A total of four isopach maps are generated based on the thickness between key chronostratigraphic horizons that define unique sedimentary packages at MC118. Isopach thickness was mapped for each interval using the Surfer mapping program and contours are based on an inverse square to distance algorithm. Thickness maps are converted to sedimentation rate maps for each isopach interval using age control provided by biostratigraphy and radiocarbon dating (Sections 3.4–3.6).

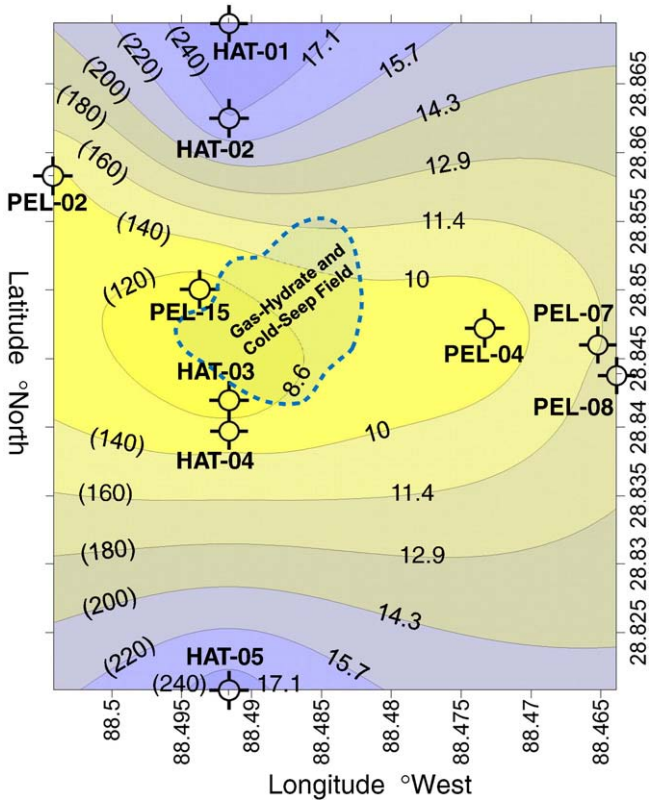

Fig. 7. Isopach thickness and sedimentation rate map of the MC118 area for the interval above the red band, ~14 kilo-yrs BP to the present (core tops), which includes sediments of stratigraphic Units I and II. Very shallow latest Holocene sediments may be missing in some cores. Core locations are identified by open circles. The area of the present-day gas-hydrate–cold-seep field is indicated by the transparent blue shading within the dotted outline. Contour lines are labeled using sedimentation rate (cm/yr) and thickness (cm) shown in parentheses.

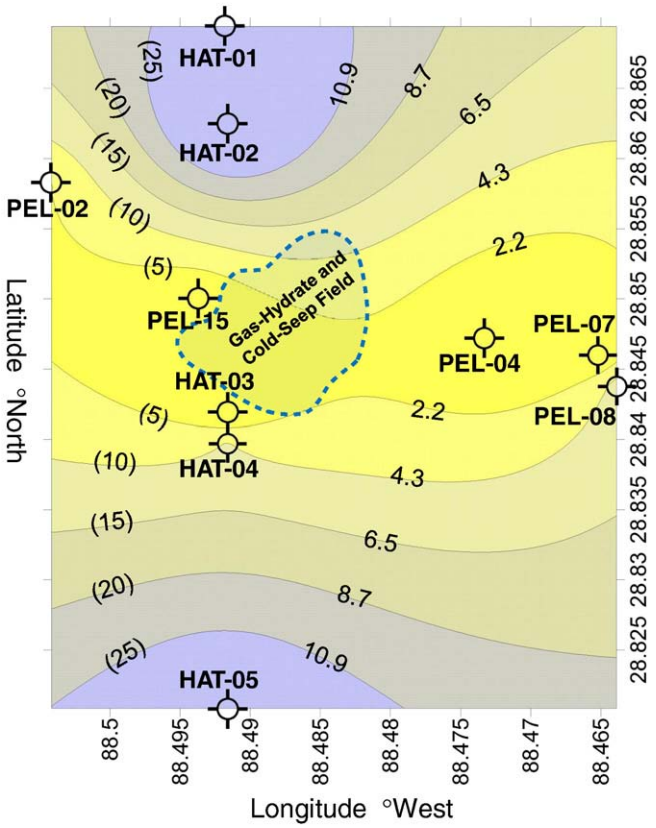

Fig. 8. Isopach thickness and sedimentation rate map of the MC118 area for the interval from ~2.3 kilo-yrs BP to present (Unit IA). These very shallow sediments are only distinguishable with the aid of XRF core scanning and are partially missing in some cores. Core locations are identified by open circles. The area of the present-day gas-hydrate–cold-seep field is indicated by the transparent blue shading within the dotted outline. Contour lines are labeled using sedimentation rate (cm/yr) and thickness (cm) shown in parentheses.

4. Results

Analyses of the MC118 sediment cores (Table 1; Figs. 3–5) identify three distinct stratigraphic intervals that are continuous across the entire study area. These stratigraphic units are similar in overall character to those previously documented within the study area (Lutken et al., 2006; Brunner, 2007a), and in a piston core ~90 km to the west of the field recovered from the western flank of the Mississippi Canyon bathymetric feature (Brunner, 2007b). The thickness of several stratigraphic units discussed below is also represented by isopach reconstructions (Figs. 7–10).

4.1. Stratigraphic Unit I

This stratigraphic interval is the shallowest unit observed in all of the collected cores. The unit is primarily uniform calcareous nannofossil silty clay, with abundant foraminiferal microfossils and exhibits a high Ca/Ti ratio (Figs. 3–5). Both XRF core scanning (e.g., Figs. 4 and 5) and visual appearance (e.g., Fig. 3) indicate that this is the most $CaCO_3$-rich interval sampled. The color is light olive gray, visually lighter than sediments at greater depth. Sediments of Unit I appear homogenous and contain little sedimentary structures.

Stratigraphic Unit I is particularly well identified by the XRF Ca/Ti core scanning data, and is Holocene (~9500 calendar yrs BP to present) in age based on AMS radiocarbon dating (Figs. 3–5; Table 2). Foraminiferal biostratigraphic data further constrains the age of this stratigraphic unit. Core Hat-03 contains the Y/Z Subzone boundary, positioned at 60–70 cm sub-bottom depth, approximately 20 cm below the onset of the Ca/Ti peak. This places sediments above this position within the Holocene, dated to ~10 kilo-yrs BP using biostratigraphy (e.g., Flower and Kennett, 1990; Poore et al., 2003).

Unit I is defined to encompass the entire interval from the base of Ca/Ti peak to the core tops (Fig. 4), and is informally divided into two subunits: an upper interval that is laterally discontinuous (Unit IA), and a lower laterally continuous interval represented by a broad Ca/Ti peak (Unit IB). Unit IA is calcareous ooze that is late Holocene in age (~2300 calendar yrs BP to present; e.g., Fig. 4). These sediments are similar to the subjacent $CaCO_3$-rich sediments (Unit IB) and the contact between them is visually gradational making distinction difficult. However, these sediments are clearly distinguishable with the aid of XRF core scanning. Ca/Ti values of this most shallow interval (Unit IA) are low relative to the $CaCO_3$-rich interval (Unit IB), yet exhibit higher Ca/Ti values than mud-rich sediments at depth (Units II and III; Figs. 4 and 5). The top of some cores also preserve a second minor Ca/Ti peak within Unit IA (e.g. see HAT-02 and HAT-05). The very shallow sediments of Unit IA, though discontinuous, provide yet another correlative horizon at the site. Thickness and sedimentation rate maps for Units IA and IB sediments are based on the ~2300 calendar yr datum placed at the end of the sub-adjacent Ca/Ti peak (Unit IB), and extended to the core tops (Figs. 8 and 9).

4.2. Stratigraphic Unit II

This unit is a mottled hemipelagic nannofossil silty clay, and the stratigraphic top of the unit ranges from as shallow as 10 cm to as deep as 140 cm below seafloor (Fig. 3). The base of the unit extends from ~100 cm depth in some cores to over 200 cm in others (Fig. 3).

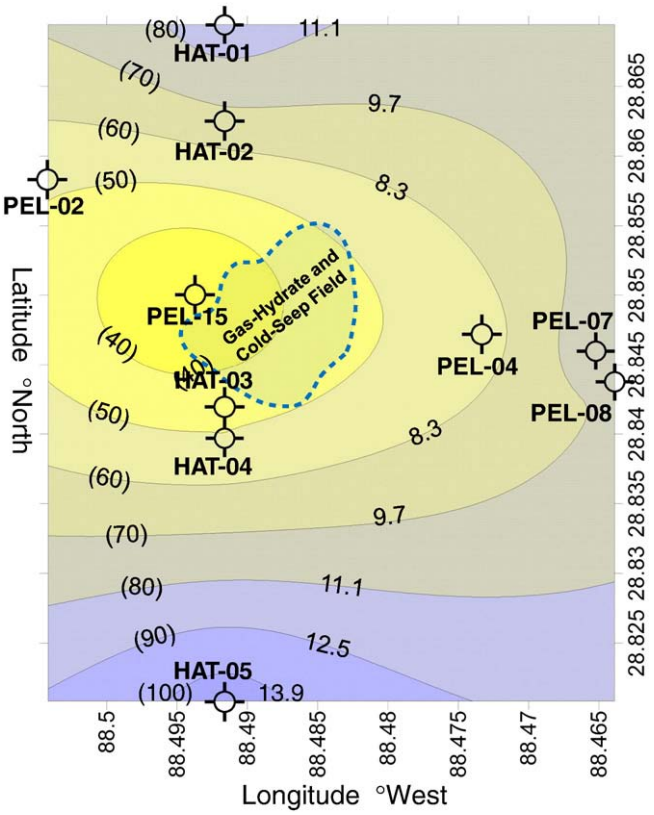

Fig. 9. Isopach thickness and sedimentation rate map of the MC118 area from the top to the base of the $CaCO_3$-rich interval of stratigraphic Unit IB, ~9.5 to ~2.3 kilo-yrs BP, identified by the Ca/Ti data, and visually by its light olive gray color. Core locations are identified by open circles. The area of the present-day gas-hydrate–cold-seep field is indicated by the transparent blue shading within the dotted outline. Contour lines are labeled using sedimentation rate (cm/yr) and thickness (cm) shown in parentheses.

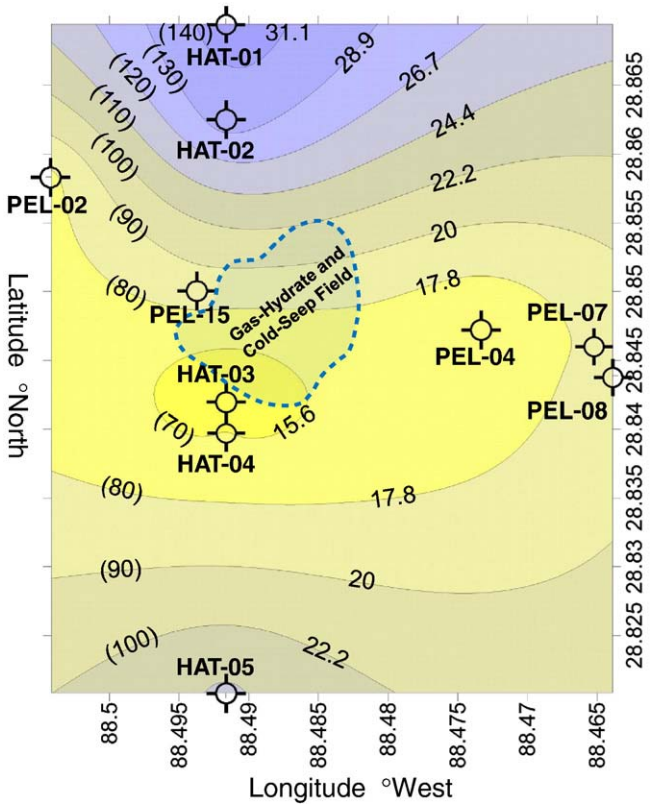

Fig. 10. Isopach thickness and sedimentation rate map of the MC118 area for Unit II, from the base of the $CaCO_3$-rich interval of Unit I, ~9.5 kilo-yrs BP, to the red band interval, ~14 kilo-yrs BP, marking the top of Unit III. Core locations are identified by open circles. The area of the present-day gas-hydrate–cold-seep field is indicated by the transparent blue shading within the dotted outline. Contour lines are labeled using sedimentation rate (cm/yr) and thickness (cm) shown in parentheses.

This unit displays visual mottling of dark olive brown colors and light olive gray colors with tubular structures (resembling borrows). The color mottling is observed in each core, and gradually decreases with depth to the base of the unit.

XRF core scans indicate that Unit II sediments are markedly more mud-rich, displaying low Ca/Ti ratios (Figs. 4, 5, and 10). The stratigraphic top of the unit is defined by an increase in Ca/Ti values associated with the more $CaCO_3$-rich Unit I (Figs. 4 and 5) and its base is defined by the first distinct presence of reddish banding (Figs. 3–5, see Section 4.3). Its age ranges between 9500 yrs and 15,500 calendar yrs BP based on radiocarbon and nannofossil biostratigraphy (Marchitto and Wei, 1995; Figs. 3–6). Chronologic constraint thus indicates that these sediments represent the late Pleistocene to earliest Holocene transition.

4.3. Stratigraphic Unit III

Sediments of Unit III are well-laminated hemipelagic nannofossil silty clay, olive to dark olive brown in color, containing numerous reddish bands that increase in frequency with depth (Fig. 3). In places, Unit III exhibits irregular contacts across the reddish bands. The top of the unit is marked by a single distinctive red band of nannofossil silty clay that varies in depth from 115 cm below seafloor in Core HAT-03 to 255 cm below seafloor in Core HAT-05 (Fig. 3). Evaluation of the abundance of pre-Quaternary nannofossils at MC118 indicates that the position of this red band closely corresponds to the first peak in reworked nannofossils (Figs. 3–6). Several cores exhibit a double peak of pre-Quaternary nannofossils across the red band interval. Core HAT-01 lacks the highly reworked nannofossil peak, the red band, or clear laminations, indicating the absence of Unit III sediments (Figs. 3 and 4).

Marchitto and Wei (1995) described an increase in reworked nannofossil abundance in sediments from the Orca Basin during meltwater pulse 1a (Fig. 6; see Discussion). Supporting chronologic constraints validate correlation of the reworked nannofossil peak observed in the Orca Basin and MC118 (e.g., Marchitto and Wei, 1995; Fig. 6). Using the chronology of Marchitto and Wei (1995) from the Orca Basin (Fig. 6), the stratigraphic top of Unit III is approximately 14 kilo-yrs.

Foraminiferal biostratigraphy indicates that the Y_1/Y_2 subzone boundary, ~15 kilo-yrs BP is between 120 and 122 cm below sea floor (cmbsf) in Core HAT-03, just below the red band and the reworked nannofossil peak. Sediments of Unit III are at least latest Pleistocene in age, and no younger than 14 Ka based on nannofossil biostratigraphy, 15 Ka based on foraminiferal biostratigraphy, and 15.5 Ka based on radiocarbon dating (Table 2, Fig. 3). Stratigraphic Unit III lacks a clear basal horizon across the study area; hence, neither the total thickness nor the average sedimentation rate can be determined for these latest Pleistocene sediments.

5. Discussion

The results of this study indicate pronounced changes in sedimentation at MC118 during the latest Pleistocene–Holocene, with respect to the rate and pattern of deposition, as well as the geochemistry of the sediments. This is well documented by the observed variability in XRF-scanning Ca/Ti profiles. Sedimentologic

Table 2
AMS radiocarbon dating of planktonic foraminifera at MC118.

Core I.D.	Sub-bottom depth (cm)	Radiocarbon age (yr)	Gulf of Mexico reservoir correction	Calendar-age reservoir corrected (yBP)	Error (yr)
HAT-02	12	1270	870	773	47
	25	1940	1540	1418	53
	50	2720	2320	2336	22
	120	10,300	9900	11,280	56
	245	13,750	13,350	15,544	121
	265	14,100	13,700	15,946	132
HAT-03	10	2550	2150	2146	66
	30	4190	3790	4162	48
	115	11,650	11,250	13,086	67
	270	16,450	16,050	19,182	103
HAT-04	20	2870	2470	2565	90
HAT-05	6	1460	1060	960	25
	20	1780	1380	1296	28
	120	8920	8520	9513	21
PEL-15	4	3210	2810	2901	39
	30	9660	9260	10,441	91
	453	15,800	15,400	18,632	98
PEL-04	4	1480	1080	978	38
	40	7660	7260	8067	55
	406	15,200	14,800	17,702	216

List of AMS dates from "picked" foraminifera indicating, the location (depth) of the sample in each core, radiocarbon years, reservoir correction, reservoir-corrected age and error. Note: Core Hat-03, with a sample depth of 115 cm, is anomalously young by approximately 1000 calendar yrs, and thus is not utilized in the final chronostratigraphy. Error in calendar years is 1 standard deviation.

observations from the MC118 cores indicate that increases in carbonate content are primarily attributable to an increase in the abundance of microfossils (e.g., foraminifers and nannofossils), and thus elevated calcium concentration in MC118 sediments is primarily attributable to an increase in biogenic $CaCO_3$ (Brunner, 2007a, b). Terrigenous contributions are inferred from the relative abundance of titanium, supplied to the Gulf of Mexico shelf and slope from lithogenic sources and primarily derived from ilmenite ($FeTiO_3$), closely followed by rutile (TiO_2), minerals mostly associated with sand- and silt-size grains (Woolsey, 1984; Appelbaum and Bouma, 1972). Hence, in the Gulf of Mexico, the Ca/Ti ratio generally reflects relative changes in biogenic verses lithogenic sedimentation.

The most obvious geochemical feature in sediments from MC118 is elevated $CaCO_3$ concentration from 2300 to 9500 calendar yrs BP (Unit IB, Ca/Ti peak; Figs. 4 and 5). The onset of this $CaCO_3$-rich sedimentation may largely represent decreased silt and clay flux associated with Holocene sea-level rise and retreat of the shoreline. Holocene delta lobe switching provides a second mechanism to explain observed trends in biogenic carbonate versus lithogenic components of sedimentation at the MC118 site. The timing and relative positions of the Holocene Mississippi River deltaic lobes have been previously considered in several investigations (Törnqvist et al., 1996; Roberts, 1997; Aharon 2006; Blum and Roberts, 2009), and show consistency with the Ca/Ti data from MC118. For example, during the period from 7500 to 5000 calendar yrs BP, the early Holocene Louisiana deltas prograded far to the west, approximately 300 km from the modern Mississippi River outflow (Blum and Roberts, 2009). The positioning of the delta at that time is coincident with $CaCO_3$-rich sedimentation at MC118, suggesting that the location of the delta to the west diminished terrigenous sedimentation at MC118. A third interpretation is that of elevated biological $CaCO_3$ production during the deposition of Unit IB, and consequent dilution of the lithogenic components. However, a reduction in sedimentation rate at MC118 from the latest Pleistocene to Holocene transition (Section 5.1; Figs. 7–10) argues against the hypothesis of enhanced biological production. Hence, past sea-level change and movement of the Mississippi Delta seem to be the most likely explanation for the observed changes in the Ca/Ti ratio.

Deltaic shifting to the east (towards MC118) by the Teche delta complex (5.5–3.5 Ka) and especially the St. Bernard delta complex (4.0–2.0 Ka), should have resulted in an increase in lithogenic sedimentation at MC118 (Blum and Roberts, 2009). Consistent with this, we observe a decrease in the Ca/Ti ratio commencing by at least 2.9 Ka (see PEL-15 in Fig. 5). This interval is followed at the very top (<20 cmbsf) in Cores HAT-02 and HAT-05 by a short-lived Ca/Ti peak (Fig. 4), perhaps marking higher frequency changes in the Mississippi River outflow. The general position of the modern Plaquemines–Balize delta and Mississippi River mouth was established by 1.3 Ka, and reaches directly toward the MC118 study area. This positioning likely contributes to lithogenic dilution of carbonate content at the very top of the MC118 cores.

5.1. Isopach mapping

The stratigraphic intervals observed at MC118 are summarized and mapped by isopach thickness and associated sedimentation rate (e.g., Figs. 7–10). These maps reveal an overall decrease in sedimentation rate from ~14 Ka to present, yet spatial patterns of deposition surrounding the field are consistent across all intervals (Figs. 7–10). The general pattern of sedimentation at MC118 is summarized by an isopach from the red band at the top of Unit III (~14 Ka) to the present, indicating stratigraphic thickening and elevated sedimentation rate with distance from the field (Fig. 7). The shallowest isopach exhibits a similar pattern (Unit IA; Fig. 8), as does the Holocene $CaCO_3$-enriched interval (Unit IB; 2.3–9.5 Ka; Fig. 9), and the mottled nannofossil silty clay of Unit II (9.5–14 Ka; Fig. 10).

The isopach map reconstructions indicate that the location of stratigraphic thinning (adjacent to the gas-hydrate/cold-seep field) shifts from a more offshore position during the latest Pleistocene–Early Holocene (14 to 9.5 Ka; Fig. 10) to a more landward location during the Holocene (Unit IB; 2.3–9.5 Ka; Fig. 9). This observation is suggestive of migration of fluid seepage and hydrate activity along the seafloor in a northward upslope direction from the latest Pleistocene to the Holocene. The change in position of stratigraphic thinning through time may be a result of subtle changes in bathymetry and movement of paleo-highs induced by seafloor warping from subsurface salt, potentially including alteration of the subsurface plumbing. Cold seeps and mud volcanoes alike can shift their position through time and this phenomenon has been observed in terrestrial mud volcanoes that produce numerous mounds and craters that collapse, change shape, and shift position (Dimitrov, 2002). On a localized

scale, the seafloor near the MC118 gas vents and petroleum seeps exhibit slight depressions and craters (Figs. 1 and 2), although the density of coring does not permit evaluation of sedimentation trends inside the field. It should be emphasized that sedimentation controlled by salt tectonics is important on geologic timescales and ultimately is a key factor in controlling deposition along the Gulf of Mexico continental slope (Galloway et al., 2000; Winker and Booth, 2000; Diegel et al., 1995; Jackson, 1995). Complex interactions between subsurface salt deposits, fluid migration and sedimentation seem likely at MC118.

Shifting of the MC118 field due to changes in hydrate stability associated with rising sea level is an alternative hypothesis to explain observations, but is not consistent with theoretical prediction. The MC118 site has remained at sufficient water depth and beneath the zone of potential methane-hydrate instability since the Late Pleistocene as predicted by stability in seawater (e.g., 400–600 m water depth; Lerche and Bagirov, 1998; Dickens and Quinby-Hunt, 1994), however, advection of warm fluids from the subsurface complicate the base of the hydrate stability zone. Furthermore, gas hydrate at the MC118 site formed in close proximity to petroleum seepage, which hosts a mixture of thermogenic gases, and therefore is more stable than pure methane hydrate (e.g., Lerche and Bagirov, 1998; Sassen et al., 2001).

Finally, the similarity of Cores HAT-02 and HAT-05 is striking (Fig. 4; Figs. 7–10) with respect to the shape of the Ca/Ti profiles and thickness of each interval, suggesting that these sites record undisturbed background sedimentation. In total, the results of this study are consistent with remobilization of sediment or reduced sedimentation over the gas-hydrate/cold-seep field, yet are not suggestive of significant seafloor failure across this area (1005 of meters) during the past ~14,000 yrs. However, given the location of the core sites outside the field, it is difficult to detect localized (meter-scale) remobilization events (e.g., Figs. 1 and 2).

5.2. The "red band"

The reddish-colored interval ("red band") that defines the top of Unit III has previously been observed at MC118 (Lutken et al., 2006; Brunner, 2007a; Sleep et al., 2008). The red band level is generally contemporaneous with the most recent interval of reworked nannofossils (also typically the highest magnitude peak of reworked nannofossils; Figs. 4–6). Although no unique elemental composition was observed across the red band, it is, however, associated with a negative $\delta^{18}O$ excursion from a series of planktonic foraminifera samples from Core HAT-03 (W. Ingram, unpublished data). Marchitto and Wei (1995) also discovered a similar coincidence of highly reworked nannofossils and strongly negative $\delta^{18}O$ isotopic values from planktonic foraminifera, which they attributed to scouring of epicontinental sediments by glacial meltwater outflow down the Mississippi River drainage basin and into the Gulf of Mexico.

It is possible that highly weathered, subaerially exposed sediments spanning the midcontinent of North America were delivered to MC118 by meltwater discharge events that drained large pro-glacial lakes as described by Marchitto and Wei (1995). Interestingly, the frequency of red banding increases with depth below the initial, most prominent red band that defines the top of stratigraphic Unit III. At these depths, well below the initial red band, sediments are most certainly latest Pleistocene, up to ~19,000 calendar yrs BP, based on radiocarbon dating (Figs. 3–5). The chronostratigraphy developed in this study indicate latest Pleistocene laminated sediments were deposited rapidly and were perhaps derived from weathered, subaerially exposed and oxidized sediments of the North American midcontinent, bypassing the shelf during the latest Pleistocene sea-level low stand. Constans and Parker (1986) have established the percentage of reworked (extinct) nannofossils as a proxy indicator for enhanced erosion of terrestrial epicontinental sediments and subsequent delivery to the continental slope of the northern Gulf of Mexico during sea-level low stands on glacial–interglacial cycles. Nannofossil biostratigraphic results of this study suggest similar processes were involved during the time the red band interval was deposited. Additionally, previous investigators (e.g., Aharon 2006) have suggested hyperpycnal flow of meltwater into the Gulf of Mexico during the period from 14.7 to 14.2 calendar kilo-yrs coincident with the timing of the red band at MC118. Thus the observed red band may represent a proxy indicator for a significant erosional event perhaps connected to the draining of large terrestrial pro-glacial lakes and the delivery of oxidized sediments to the Gulf of Mexico. Although the proposed hypothesis for the formation of the red band is speculative, this interval is nonetheless highly continuous in sediments around the MC118 study area. Hence, the red band provides a new chronostratigraphic marker for sediments in the vicinity of MC118.

6. Conclusions

This study establishes a chronostratigraphic framework for late Pleistocene–Holocene sedimentation surrounding the MC118 gas-hydrate and cold-seep field. The results provide compelling evidence for enhanced sediment erosion, remobilization and/or non-deposition in close proximity to the MC118 field. Isopach reconstructions clearly indicate greater stratigraphic thickness and higher sedimentation rates with distance from the gas-hydrate/cold-seep field. The evolution of sedimentation patterns over the past 14 Ka reveals lateral shifting in the position of stratigraphic thinning, which likely reflects migration of the locus of hydrate outcropping and cold seepage and/or movement of subtle paleo-bathymetric highs through time. The ultimate cause of the observed stratigraphic patterns likely involves complex interactions between subsurface salt deposits, fluid migration and sedimentation.

The MC118 stratigraphic record reveals similar sedimentation and bulk geochemistry far upslope and downslope from the field. This result is inconsistent with catastrophic slope failure or major disruptions to sedimentation over a large portion of the seafloor at MC118, at least since the end of the last deglacial. Changes in the sedimentation rate and consistent variability in geochemistry through time at MC118 at each core site is most likely a consequence of deglacial sea-level rise and regional factors such as Mississippi delta lobe switching.

Acknowledgements

This research was supported with funding from the Gulf of Mexico Gas Hydrate Research Consortium (HRC grants 300212198E (UM 07-01-071) and 300212260E (UM 08-11-047) to C.S. Martens). Funding for ship time on the *R/V Pelican* was provided by Minerals Management Services and NOAA's National Institute for Undersea Science and Technology. Funding for the *R/V Hatteras* Cruise, ship time and coring operations was provided by the Duke/UNC Oceanographic Consortium as part of a joint proposal with other UNC investigators, Kai Ziervogel, Drew Steen and Carol Arnosti. The crew, joint investigators listed above, Sherif Ghobrial, Carol Lutken and Ken Sleeper were all instrumental in the shipboard core collection process that provided the material used for this study. Joe Forest provided assistance with using the Surfer program to construct isopach maps.

References

Aharon, P., 2006. Entrainment of meltwaters in hyperpycnal flows during deglaciation superfloods in the Gulf of Mexico. Earth and Planetary Science Letters 241 (1–2), 260–270.

Appelbaum, B.S., Bouma, A.H., 1972. Geology of the upper continental slope in the Alaminos Canyon region. Gulf Cost Association of Geological Societies Transactions 22, 157–164.

Blum, M.D., Roberts, H.H., 2009. Drowning of the Mississippi Delta due to insufficient sediment supply and global sea-level rise. Nature Geoscience 2, 488–491.

Broecker, W.S., Andreé, M., Wolfli, W., Oeschger, H., Bonani, G., Kennett, J.P., Peteet, D., 1988. The chronology of the last deglaciation: implications to the causes of the Younger Dryas event. Paleoceanography 3, 1–19.
Broecker, W.S., Kennett, J.P., Flower, B.P., Teller, J.T., Trumbore, S., Bonani, G., Wolfli, W., 1989. Routing of meltwater from the Laurentide ice sheet during the Younger Dryas cold episode. Nature 341, 318–321.
Brunner, C.A., 2007a. Stratigraphy and paleoenvironment of shallow sediments from MC118. Proceedings of the Annual Meeting of the Gulf of Mexico Hydrates Research Consortium, October 10–11, 2007, Oxford, Ms. [one CD].
Brunner, C.A., 2007b. Qualitative planktonic foraminiferal biostratigraphy of core MD02-2570, of late Quaternary age, from the northern Gulf of Mexico. In: Winters, W.J., Lorenson, T.D., Paull, C.K. (Eds.), Initial report of the gas hydrate and paleoclimate cruise on the R/V *Marion Dufresne* in the Gulf of Mexico, 2–18 July 2002: USGS Open-File Report 2004-1358, one DVD. online at http://www.pubs.usgs.gov/of/2004/1358/.
Castellini, D.G., Dickens, G.D., Snyder, G.T., Ruppel, C.D., 2006. Barium cycling in shallow sediments above active mud volcanoes in the Gulf of Mexico. Chemical Geology 226, 1–30.
Constans, R.E., Parker, M.E., 1986. Calcareous nannofossil biostratigraphy and paleoclimate indices for the Late Quaternary, Deep Sea Drilling Project Leg 96, Gulf of Mexico. In: Bouma, A.H., Coleman, J.M., Meyer, A.W., et al. (Eds.), Initial Reports of the Deep Sea Drilling Project 96. U.S. Government Printing Office, Washington, D.C., pp. 601–630.
Dickens, G.R., Quinby-Hunt, M.S., 1994. Methane hydrate stability in seawater. Geophysical Research Letters 21, 2115–2118.
Dickens, G.R., Castillo, M.M., Walker, J.C.G., 1997. A blast of gas in the latest Paleocene: simulating first-order effects of massive dissociation of methane hydrate. Geology 25, 259–262.
Diegel, F.A., Karlo, J.F., Schuster, D.C., Shoup, R.C., Tauvers, P.R., 1995. Cenozoic structural evolution and tectono-stratigraphic framework of the northern Gulf Coast continental margin, in: Jackson, M.P.A., Roberts, D.G., Snelson, S., (Eds.), Salt Tectonics: A Global Perspective: American Association of Petroleum Geologist Memoir 65, pp. 109–151.
Dimitrov, L.I., 2002. Mud volcanoes—the most important pathway for degassing deeply buried sediments. Earth Science Reviews 59, 49–76.
Fairbanks, R.G., Mortlock, R.A., Chiu, T.-C., Cao, L., Kaplan, A., Guilderson, T.P., Fairbanks, T.W., Bloom, A.L., Grootes, P.M., Nadeau, M.-J., 2005. Radiocarbon calibration curve spanning 0 to 50, 000 years BP based on paired 230Th/234U/238U and 14C dates on pristine corals. Quaternary Science Reviews 24, 1781–1796.
Flower, B.P., Kennett, J.P., 1990. The Younger Dryas cool episode in the Gulf of Mexico. Paleoceanography 5 (6), 949–961.
Galloway, W.E., Ganey-Curry, P.E., Li, X., Buffler, R.T., 2000. Cenozoic depositional history of the Gulf of Mexico basin. American Association of Petroleum Geologists Bulletin 84 (11), 1743–1774.
Haq, B.U., 1998. Natural gas hydrates: searching for the long-term climatic and slope-stability records. In: Henriet, J.P., Mienert, J. (Eds.), Gas Hydrates: Relevance to World Margin Stability and Climate Change: Geological Society, London Special Publications, 137, pp. 303–318.
Jackson, M.P.A., 1995. Retrospective Salt Tectonics, in: M.P.A. Jackson, D.G. Roberts, S. Snelson, (Eds.), Salt Tectonics: a Global Perspective. AAPG Memoir 65, pp. 1–28.
Katz, M.E., Pak, D.K., Diskens, G.R., Miller, K.G., 1999. The source and fate of massive carbon input during the latest Paleocene thermal maximum. Science 286, 1531–1533.
Kennett, J.P., Huddlestun, P., 1972. Late Pleistocene paleoclimatology, foraminiferal biostratigraphy and tephrochronology, Western Gulf of Mexico. Quaternary Research 2, 38–69.
Kennett, J.P., Elmstrom, K., Penrose, N.L., 1985. The last deglaciation in Orca Basin, Gulf of Mexico: high-resolution planktonic foraminifera changes. Paleogeography, Paleoclimatology, Paleoecology 50, 189–216.
Kennett, J.P., Cannariato, K.G., Hendy, I.L., Behl, R.J., 2000. Carbon isotopic evidence for methane hydrate instability during Quaternary interstadials. Science 288 (5463), 128–133.
Kennett, J.P., Cannariato, K.G., Hendy, I.L., Behl, R.J., 2003. Methane Hydrates in Quaternary Climate Change: The Clathrate Gun Hypothesis. American Geophysical Union, Washington, DC. 216 pp.
Lapham, L.L., Chanton, J.P., Martens, C.S., Sleeper, K., Woolsey, J.R., 2008. Microbial activity in surficial sediments overlying acoustic wipeout zones at a Gulf of Mexico cold seep. Geochemistry, Geophysics, Geosystems 9 (4), 1–17.
Lapham, L.L., Chanton, J.P., Chapman, R., Martens, C.S., (in press). Methane undersaturated fluids in deep-sea sediments: implications for gas hydrate stability and rates of dissolution. Manuscript for Earth and Planetary Science Letters
Lerche, I., Bagirov, E., 1998. Guide to gas hydrate stability in various geological settings. Marine and Petroleum Geology 15 (5), 427–437.
Lutken, C.B., Brunner, C.A., Lapham, L.L., Chanton, J.P., Rogers, R., Sassen, R., Dearman, J., Lynch, L., Kuykendall, J., Lowrie, A., 2006. Analyses of core samples from Mississippi Canyon 118, paper OTC 18208, Offshore Technology Conference, American Association of Petroleum Geologist, May 1–4, Houston, TX.
Marchitto, T.M., Wei, K.-Y., 1995. History of the Laurentide meltwater flow to the Gulf of Mexico during the last deglaciation, as revealed by reworked calcareous nannofossils. Geology 23, 779–782.
Maslin, M., Mikkelsen, N., Vilela, C., Haq, B., 1998. Sea-level and gas-hydrate-controlled catastrophic sediment failures of the Amazon Fan. Geology 26 (12), 1107–1110.
Maslin, M., Owen, M., Day, S., Long, D., 2004. Linking continental-slope failures and climate change: testing the clathrate gun hypothesis. Geology 32, 53–56.
McGee, T., 2006. A seafloor observatory to monitor gas hydrates in the Gulf of Mexico. The Leading Edge 25 (5), 644–647.
Mienert, J., Vanneste, M., Bunz, S., Andreassen, K., Haflidason, H., Sejrup, H.P., 2005. Ocean warming and gas hydrate stability on the mid-Norwegian Margin at the Storegga Slide. Marine and Petroleum Geology 22, 233–244.
Milkov, A.V., Sassen, R., 2002. Thickness of gas hydrate stability zone, Gulf of Mexico, continental slope. Marine and Petroleum Geology 17, 981–991.
Paull, C.K., Brewer, P.G., Ussler III, W., Peltzer, E.T., Rehder, G., Clague, D., 2003. An experiment demonstrating that marine slumping is a mechanism to transfer methane from gas-hydrate deposits into the upper ocean and atmosphere. Geomarine Letters 22, 198–203.
Paull, C.K., Buelow, W.J., Ussler III, W., Borowski, W.S., 1996. Increased continental-margin slumping frequency during sea-level lowstands above gas hydrate-bearing sediments. Geology 24 (2), 143–146.
Poore, R.Z., Dowsett, J.J., Verardo, S., 2003. Millennial- to century-scale variability in Gulf of Mexico Holocene climate records. Paleoceanography 18 (2), 1–13.
Richey, J.N., Poore, R.Z., Flower, B.P., Quinn, T.M., 2007. 1400 yr multiproxy record of climate variability from the northern Gulf of Mexico. Geology 35 (5), 423–426.
Roberts, H.H., 1997. Dynamic changes of the Holocene Mississippi river delta plain: the delta cycle. Journal of Coastal Research 13, 605–627.
Sassen, R., Sweet, S.T., Milkov, A.V., DeFreitas, D.A., Kennicutt, M.C., 2001. Thermogenic vent gas and gas hydrate in the Gulf of Mexico slope: is gas hydrate decomposition significant? Geology 29 (2), 107–110.
Sassen, R., Roberts, H.H., Jung, W., Lutken, C.B., DeFreitas, D.A., Sweet, S.T., Guinasso Jr., N.L., 2006. The Mississippi Canyon 118 gas hydrate site: a complex natural system. Paper OTC 18132, Offshore Technology Conference, May 1–4, Houston, TX.
Sleeper, K.A., Lowrie, A., Bosman, A., Macelloni, L., Swann, C.T., 2006. Bathymetric mapping and high resolution seismic profiling by AUV in MC 118 (Gulf of Mexico). Paper OTC 18133, Offshore Technology Conference, May 1–4, Houston, TX.
Sleeper, K.A., Lutken, C., 2008. Activities Report for Cruise GOM1-08-MC118 aboard the *R/V Pelican* Sampling and Deployment Cruise Mississippi Canyon Federal Lease Block 118 Northern Gulf of Mexico April 22–28, 2008. The Center for Marine Resources and Environmental Technology and the Seabed Technology Research Center, University of Mississippi. http://www.olemiss.edu/depts/mmri/programs/ppt_list.html, 16 pp.
Solheim, A., Bryn, P., Berg, K., Mienert, J., 2005. Ormen Lange — an integrated study for the safe development of a deep-water gas field within the Storegga Slide Complex, NE Atlantic continental margin. Marine and Petroleum Geology 22 (1–2), 221–318.
Stuiver, M., Polach, H.A., 1977. Discussion: reporting of ^{14}C data. Radiocarbon 19, 355–363.
Stuiver, M., 1980. Workshop on 14C data reporting. Radiocarbon 22, 964–966.
Törnqvist, T.E., Kidder, T.R., Austin, W.J., van der Borg, K., de Jong, A.F.M., Klerks, C.J.W., Snijders, E.M.A., Storms, J.E.A., van Dam, R.L., Wiemann, M.C., 1996. A revised chronology for Mississippi River subdeltas. Science 273 (5282), 1693–1696.
Winker, C.D., Booth, J.R., 2000. Sedimentary dynamics of the salt-dominated continental slope, Gulf of Mexico: integration of observations from the seafloor, near surface, and deep subsurface. GCSSEPM Foundation 20th Annual Research Conference Deep-Water Reservoirs of the World, Dec. 3–6, pp. 1059–1086.
Woolsey, J.R., 1984. Exploration for industrial minerals in Mississippi Sound and adjacent offshore territories of Mississippi and Alabama. Mississippi–Alabama Sea Grant Consortium, Project No. R/ER-11, Grant No. NA81AA-D-00050. 22 pp.